Composite Structures 354 (2025) 118786

Contents lists available at ScienceDirect

Composite Structures

journal homepage: www.elsevier.com/locate/compstruct

Equivalent plate formulation of Double–Double laminates for the gradient-based design optimization of composite structures

David Zerbst *, Lennart Tönjes, Sascha Dähne, Edgar Werthen, Erik Kappel, Christian Hühne

German Aerospace Center (DLR), Institute of Lightweight Systems, Lilienthalplatz 7, Braunschweig, 38108, Germany

ARTICLE INFO

Dataset link: https://doi.org/10.5281/zenodo.10302734

Keywords:
Composite design
Gradient-based optimization
Double–Double laminates
Lamination parameter

ABSTRACT

The Double–Double concept of composite laminates suggests huge simplifications in aerospace structural design and manufacturing. This work presents a homogenized composite formulation introducing an analytical DD equivalent plate. Additionally, an optimization strategy is proposed using the DD parameterization as design variables to derive an optimized thickness and stiffness distribution on the basis of gradient-based numerical sensitivities. The method is applied to a simple wing box benchmark model for composite design applications. Based on this model, the usage of gradients is verified for the newly implemented DD formulation with a global optimum and a robust convergence. Furthermore, the DD design is compared to a lamination parameter-based optimization of conventional Quad laminates. The DD optimized wing box shows small weight gains, due to the fact that one building block is distributed to an assembly of panels, whereas the Quad design provides individual optimality for each design region. At the same time, the proposed DD optimization process shows lower computational efforts, due to a lower amount of variables and constraints, while all laminate manufacturing constraints are implicitly fulfilled. Thus, the introduced DD formulation provides an efficient option to obtain a feasible structural design and therefore improve the maturity level for early aircraft design phases.

1. Introduction

The demand on the development of disruptive aircraft configurations to face the climate impact of growing aviation and transport requires multidisciplinary design optimization (MDO) strategies. The additional need to reduce time to market requires a high physical depth and reliability from contributing tools and modeling approaches. With respect to composite structures, increasing design maturity can be achieved by optimally designed discrete laminates in order to assess manufacturing feasibility in early design phases. This is a challenging task and only taken into account to a limited extent by conventional structural optimization processes within known MDO environments (e.g. [1,2]).

In general, the optimization of discrete stacking sequences and its continuous thickness leads to a mixed-integer problem. However, today's state of the art MDO workflows use gradient-based optimization methods [3,4]. In order to be able to provide sensitivities to an overall optimization process, this applies also for contributing disciplinary sub-components like a structural sizing tool. Today, various mono- and multidisciplinary composite optimization strategies exist, as comprehensively summarized in [5,6]. For the use of gradients, continuous design variables are required. These can be obtained introducing an equivalent plate, that represents the composite properties continuously over thickness. Here, different theories exist e.g. the ply share approach [7], polar parameter [8] or the common concept of lamination parameter (LP) [9]. A comparison of different continuous parameterization for composite structural optimization is given in [10].

One major challenge of using continuous parameter is the complexity induced through the consideration of manufacturing rules, e.g. balanced laminates and required symmetry. On the example of LP, these can be applied with constraints on the design space in order to find feasible layup solutions [11,12]. Especially, the problem of laminate blending between adjacent design regions remain a complex exercise (see e.g. [13,14]). Furthermore, as a second major challenge, the use of equivalent plate theories requires a reverse transformation into discrete layups. Therefore, a subsequent procedure is necessary to find a stacking sequence which meets the stiffness obtained from an optimized continuous parameterization. Different reverse transformation methods are proposed in literature with different limitations, for instance within the comprehensive consideration of manufacturing rules or efficiency due to the exponential growth of stacking sequence permutations,

* Corresponding author.
E-mail address: david.zerbst@dlr.de (D. Zerbst).

https://doi.org/10.1016/j.compstruct.2024.118786
Received 17 May 2024; Received in revised form 20 August 2024; Accepted 10 December 2024
Available online 17 December 2024

from the number of plies or ply orientations [15–17]. Hence, it is computationally challenging to comprehensively consider composites for MDO applications from the conceptual level up to a discrete and manufacturable structure.

Using Double–Double (DD) laminates, as suggested by [18], can overcome the above-mentioned challenges for composite design problems. The DD idea basically intends the repetition of a balanced building block comprising four unidirectional plies. This unit will be distributed over respective shell structures and repeated locally over thickness until desired design criteria are full-filled. This strategy leads to laminate homogeneity and induces mechanical simplicity in composite design and manufacturing, as comprehensively summarized in [19]. The present paper provides a computational perspective, showcasing the advantages of DD in gradient-based structural optimization. Therefore, an equivalent plate representation for DD laminates is introduced, that provides continuous design variables. The plate formulation is feasible by definition, such that additional constraints for blending and manufacturing as well as a stacking sequence reverse transformation process can be avoided. The proposed DD optimization strategy is analyzed on an academic benchmark wing box use case. Finally, the DD design is compared to a reference design using conventional Quad laminates, derived from an LP parameterization, in terms of stiffness, mass and computational performance.

2. DD laminates

2.1. Laminate architecture

The family of DD laminates has been proposed by Steve Tsai [18] as a promising challenger for the family of conventional laminates in aerospace practice, which are usually composed of the four-ply orientations $0°, \pm 45°, 90°$. Those conventional stackings are denoted as 'Quad' in DD-related literature, what is adopted hereafter. Laminate symmetry and balanced stackings are essential rules for Quad laminates, which are necessary to circumvent unwanted in-plane (shear) and out-of-plane (bending, warpage) coupling effects. Those requirements created complexity in laminate-design tasks such as stacking-sequence optimization for adjacent laminate zone.

DD laminates do not require symmetry, which is considered the most-remarkable opportunity from a manufacturing perspective. The laminate architecture differs. At the same time, laminate optimization is simplified.

A DD laminate is composed of a particular sequence of four-ply sub-laminates, which are usually denoted as building blocks (BB).

A BB consists of only four ply orientations, which is a similarity to established Quad laminates (from a design-space perspective). However, a BB in the DD concept shall be balanced in addition. Thus, only two individual ply angles (Φ and Ψ) remain to describe a DD laminate stacking. A full, 4-ply BB is therefore described by $[\pm\Phi, \pm\Psi]$.[1] A laminate is composed of multiple BBs in order to tailor the local laminate thickness according to given loads. The number of building-blocks is described by the repeat index r, leading to the laminate notation $[\pm\Phi, \pm\Psi]_{rT}$. The index T in the preceding expression denotes 'total', which follows the convention of Nettles [20] and the aforementioned publication in the context of DD. The index T also helps to clearly distinguish from the often used index 's', which indicated symmetry for Quad laminates

[1] Note, that the reduction to only two ply-angle parameters allows for particularly elegant plots of the DD (Φ, Ψ) design space, as can be seen in Figs. 6 and 7. Those, plots are valuable for composite designers. Similar plots do not exist for Quad laminates.

Thickness-normalized descriptions are usually used in the context of DD (see [18,21]). Those are deduced from the CLT's (see [20]) basic relation, as shown hereafter.

$$\underbrace{\begin{pmatrix}\{N\}\\ \{M\}\end{pmatrix} = \begin{bmatrix}[A] & [B]\\ [B] & [D]\end{bmatrix} \cdot \begin{pmatrix}\{\varepsilon^0\}\\ \{\varkappa\}\end{pmatrix}}_{\text{CLT}} \tag{1}$$

Inserting stresses and strains, as $\{\sigma^0\} = \frac{1}{t_{lam}} \cdot \{N\}$, $\{\sigma^f\} = \frac{6}{t_{lam}^2} \cdot \{M\}$ and $\{\varepsilon^f\} = \frac{t_{lam}}{2} \cdot \{\varkappa\}$, yields the normalized form.

$$\begin{pmatrix}\{\sigma^0\} \cdot t_{lam}\\ \{\sigma^f\} \cdot \frac{t_{lam}^2}{6}\end{pmatrix} = \begin{bmatrix}[A] & [B]\\ [B] & [D]\end{bmatrix} \cdot \begin{pmatrix}\{\varepsilon^0\}\\ \{\varepsilon^f\} \cdot \frac{2}{t_{lam}}\end{pmatrix}$$

$$\rightarrow \begin{pmatrix}\{\sigma^0\}\\ \{\sigma^f\}\end{pmatrix} = \begin{bmatrix}[A]/t_{lam} & [B] \cdot 2/t_{lam}^2\\ [B] \cdot 6/t_{lam}^2 & [D] \cdot 12/t_{lam}^3\end{bmatrix} \cdot \begin{pmatrix}\{\varepsilon^0\}\\ \{\varepsilon^f\}\end{pmatrix}$$

$$\underbrace{\begin{pmatrix}\{\sigma^0\}\\ \{\sigma^f\}\end{pmatrix} = \begin{bmatrix}[A^*] & [B^*]\\ 3[B^*] & [D^*]\end{bmatrix} \cdot \begin{pmatrix}\{\varepsilon^0\}\\ \{\varepsilon^f\}\end{pmatrix}}_{\text{Normalized format}} \tag{2}$$

The thickness normalization leads to the fact that all matrices have the same unit, MPa. With the laminate thickness being defined as $t_{lam} = 4 \cdot r \cdot t_{ply}$, the normalized matrices are given by

$$[A^*] = \frac{[A]}{t_{lam}}, \quad [B^*] = \frac{2 \cdot [B]}{t_{lam}^2}, \quad [D^*] = \frac{12 \cdot [D]}{t_{lam}^3}. \tag{3}$$

Thorough examination of the $[B^*], [D^*]$ explains why a DD laminate can be free of warpage and extension–bending coupling, although the laminate architecture is completely asymmetric. The matrix populations of the thickness-normalized matrices are outlined hereafter. The particular, BB-based laminate architecture creates proportionality for some elements in the ABD-matrix.

$$[A^*] \neq f(r),$$

$$[B^*] = \begin{bmatrix}\frac{1}{r} \cdot (\ldots) & \frac{1}{r} \cdot (\ldots) & \frac{1}{r} \cdot (\ldots)\\ \frac{1}{r} \cdot (\ldots) & \frac{1}{r} \cdot (\ldots) & \frac{1}{r} \cdot (\ldots)\\ \frac{1}{r} \cdot (\ldots) & \frac{1}{r} \cdot (\ldots) & \frac{1}{r} \cdot (\ldots)\end{bmatrix},$$

$$[D^*] = \begin{bmatrix}\cancel{f(r)} & \cancel{f(r)} & \frac{1}{r^2} \cdot (\ldots)\\ \cancel{f(r)} & \cancel{f(r)} & \frac{1}{r^2} \cdot (\ldots)\\ \frac{1}{r^2} \cdot (\ldots) & \frac{1}{r^2} \cdot (\ldots) & \cancel{f(r)}\end{bmatrix}. \tag{4}$$

One find that all entries of the $[B^*]$-matrix, which is responsible for extension–bending coupling of a laminate, scales proportional with $1/r$.

Both the D_{16}^* and the D_{26}^* coefficients of the normalized bending-stiffness matrix even scale proportional with $1/r^2$.

This process is denoted as homogenization. It leads to the fact that critical couplings diminish when the number of BBs (parameter r) increases. Experiments show and analyses suggest that a minimum of 3–4 BBs is a reasonable lower limit.

Assessing the process of 'homogenization' is essential, when a DD laminate is designed.

[18] proposed the homogeneity condition as :

$$\begin{aligned}|A_{ij}^* - D_{ij}^*| &< 2\% \cdot \text{Tsai},\\ |B_{ij}^*| &< 2\% \cdot \text{Tsai} \quad \text{for } i,j = 1,2,6,\end{aligned} \tag{5}$$

which refers to the 'Trace' parameter, which has been denoted as Tsai-modulus, to honor its creator. The 'Tsai' parameter is defined as:

$$\begin{aligned}'Trace' = Tsai &= Q_{11} + Q_{22} + 2 \cdot Q_{66}\\ &= \bar{Q}_{11} + \bar{Q}_{22} + 2 \cdot \bar{Q}_{66}\\ &= A_{11}^* + A_{22}^* + 2 \cdot A_{66}^*\\ &= D_{11}^* + D_{22}^* + 2 \cdot D_{66}^*\end{aligned} \tag{6}$$

It is of importance in the later presented DD laminate optimization procedure.

2.2. A comment on the DD design space

A graphical representation of the design space of a composite laminate can be made on the basis of LP, as introduced in [22]. There it is shown, that the ABD-matrix entries can be expressed as a linear combination of the material invariants $\{U\}$ and the LP $[V]$:

$$\begin{Bmatrix} A_{11} \\ A_{22} \\ A_{12} \\ A_{66} \\ A_{16} \\ A_{26} \end{Bmatrix} = t_{lam} \cdot \begin{bmatrix} 1 & V_1^A & V_2^A & 0 & 0 \\ 1 & -V_1^A & V_2^A & 0 & 0 \\ 0 & 0 & -V_2^A & 1 & 0 \\ 0 & 0 & -V_2^A & 0 & 1 \\ 0 & V_3^A/2 & V_4^A & 0 & 0 \\ 0 & V_3^A/2 & -V_4^A & 0 & 0 \end{bmatrix} \begin{Bmatrix} U_1 \\ U_2 \\ U_3 \\ U_4 \\ U_5 \end{Bmatrix} \tag{7}$$

$$\begin{Bmatrix} B_{11} \\ B_{22} \\ B_{12} \\ B_{66} \\ B_{16} \\ B_{26} \end{Bmatrix} = \frac{t_{lam}^2}{4} \cdot \begin{bmatrix} 0 & V_B & V_2^B & 0 & 0 \\ 0 & -V_1^B & V_2^B & 0 & 0 \\ 0 & 0 & -V_2^B & 0 & 0 \\ 0 & 0 & -V_2^B & 0 & 0 \\ 0 & V_3^B/2 & V_4^B & 0 & 0 \\ 0 & V_3^B/2 & -V_4^B & 0 & 0 \end{bmatrix} \begin{Bmatrix} U_1 \\ U_2 \\ U_3 \\ U_4 \\ U_5 \end{Bmatrix} \tag{8}$$

$$\begin{Bmatrix} D_{11} \\ D_{22} \\ D_{12} \\ D_{66} \\ D_{16} \\ D_{26} \end{Bmatrix} = \frac{t_{lam}^3}{12} \cdot \begin{bmatrix} 1 & V_1^D & V_2^D & 0 & 0 \\ 1 & -V_1^D & V_2^D & 0 & 0 \\ 0 & 0 & -V_2^D & 1 & 0 \\ 0 & 0 & -V_2^D & 0 & 1 \\ 0 & V_3^D/2 & V_4^D & 0 & 0 \\ 0 & V_3^D/2 & -V_4^D & 0 & 0 \end{bmatrix} \begin{Bmatrix} U_1 \\ U_2 \\ U_3 \\ U_4 \\ U_5 \end{Bmatrix} \tag{9}$$

The LP are defined as

$$\begin{aligned} V_x^A &= \frac{1}{t_{lam}} \sum_{k=1}^{N} (z_k - z_{k-1}) \cdot W_x \\ V_x^B &= \frac{1}{t_{lam}^2} \sum_{k=1}^{N} (z_k^2 - z_{k-1}^2) \cdot W_x \\ V_x^D &= \frac{4}{t_{lam}^3} \sum_{k=1}^{N} (z_k^3 - z_{k-1}^3) \cdot W_x \end{aligned} \tag{10}$$

z_k is the distance of the kth-ply from the laminate mid-plane. The respective trigonometric identity W_x denotes with

$$W_x = \begin{cases} \cos(2\theta_k), & x = 1 \\ \sin(2\theta_k), & x = 2 \\ \cos(4\theta_k), & x = 3 \\ \sin(4\theta_k), & x = 4 \end{cases} \tag{11}$$

The design space of the DD laminate family is shown as projections of 2D LP combinations in Fig. 1 and compared to the design space, that is covered by symmetric Quad laminates with 0°, ±45° and 90° plies only. The DD design space is slightly wider for membrane and bending properties, represented by the $V_2^{A,D} - V_1^{A,D}$-projections, covering the whole range of ply orientations. However, it has to be noted that the convex hull approach used to plot the feasible domain [12] neglects two parabolic regions at the upper bound which cannot be covered by DD (see [23]). Significant differences also occur in V^D over V^A sections. It reflects the tied coupling of A and D matrix, due to the homogenization of DD (Eq. 4), resulting into a smaller design space. This reduces complex composite behavior, as already mentioned before in Section 2.1. In turn, the "tear-drop"-shaped design space of Quad provides options for aeroelastic tailoring, due to the fact that inhomogeneous laminates are allowed.

However, using inhomogeneous laminates differ from established practice in industrial applications. Furthermore, for conventional laminates additional stacking rules are applied, like adding a minimum of 10% of each layer orientation, requiring not more than 45° deviation between neighbors etc. (see e.g. [24]), which further reduces the Quad design space.

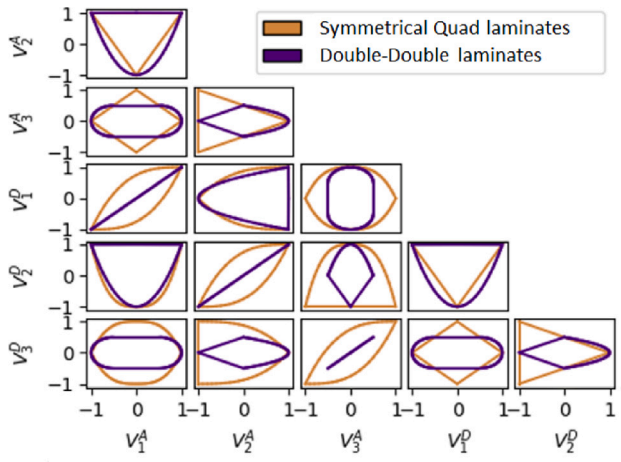

Fig. 1. Comparison of the feasible region of Quad laminates and DD in LP space.

3. DD - design approach

3.1. An equivalent plate for DD laminates

The given homogeneity over the DD laminate thickness, as outlined in Section 2.1, is the key property that enables continuous design variables for numerical sensitivities. Therefore, an equivalent plate can be formulated representing the stiffness properties of DD based on the DD angles and the plate thickness. The implemented procedure uses only one representative BB and its two independent angles Φ and Ψ (Fig. 2). The BB constitutive properties are composed by the transformed reduced stiffnesses $[\bar{Q}]$ of four plies k, given with

$$[\bar{Q}]_k = [T]_k^{-1} [Q] [T]_k \tag{12}$$

with the transformation matrix $[T]_k$ being

$$[T]_k = \begin{bmatrix} \cos^2(\theta) & \sin^2(\theta) & 2\sin(\theta)\cos(\theta) \\ \sin^2(\theta) & \cos^2(\theta) & -2\sin(\theta)\cos(\theta) \\ -\sin(\theta)\cos(\theta) & \sin(\theta)\cos(\theta) & \cos^2(\theta) - \sin^2(\theta) \end{bmatrix} \tag{13}$$

and θ taking angles $[-\Phi, \Psi, \Phi, -\Psi]$ for $k = 1...4$.

This BB now provides the in-plane stiffness $[A]$, which is independent of the amount of repetitions, using $[\bar{Q}]_k$ of the four plies contributing with a proportion of $t_{lam}/4$ each.

$$[A] = \sum_{k=1}^{4} \left([\bar{Q}]_k \cdot \frac{t_{lam}}{4} \right) \tag{14}$$

With the assumption of homogeneity and coupling terms being 0, due to sufficient repetitions, the $[D]$ matrix is then set to

$$[D] := \frac{t_{lam}^2}{12} \cdot [A] \tag{15}$$

and the $[B]$ matrix is set to 0. This way, the stiffness can be adjusted using only three design variables per optimization region.

One major advantage of a DD design is that continuous plies over adjacent panels are always given, which avoids the problem of laminate blending. For the design optimization, that means that the DD angles Φ and Ψ are the same for all BB plies of one assembly, like wing covers or spars. The optimized combination is a compromise between all panels, while the thicknesses t_{lam} can be adjusted individually. With this procedure the design problem is further reduced, but in turn the composite design is less specific, which effects the structural mass.

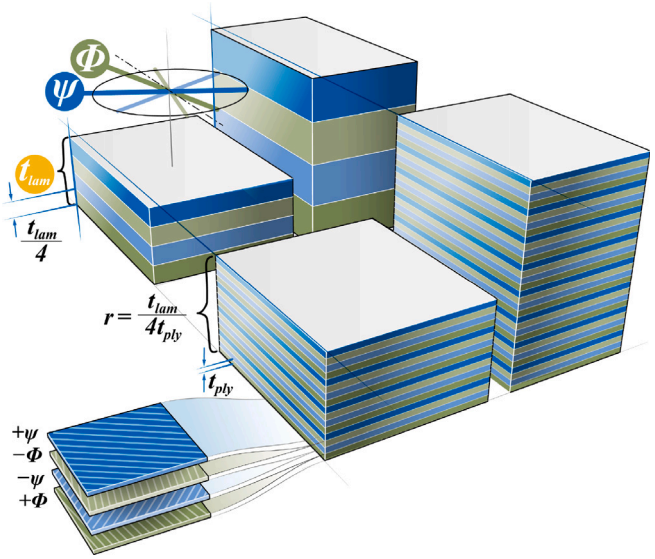

Fig. 2. Illustration of the implemented DD parameterization from continuous (back) to discrete (front).

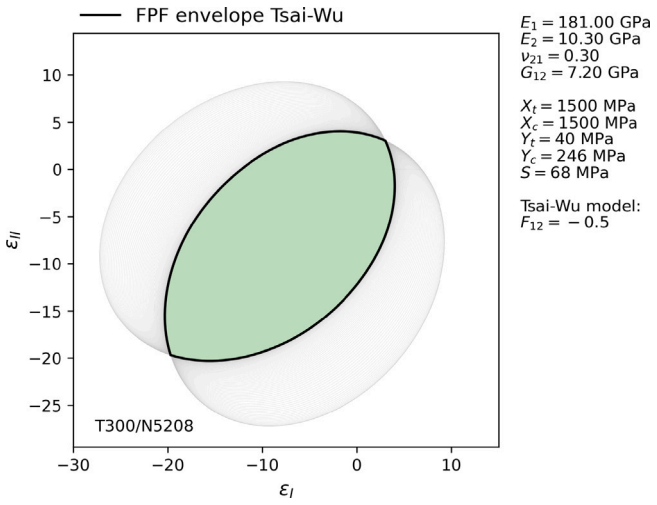

Fig. 3. Omni-FPF envelope for T300/N5208 material using Tsai–Wu criterion. Principal strains shown in ‰.
Source: Data from [27].

3.2. Stacking sequence retrieval

The derivation of a discrete stacking from optimized continuous design regions, that fulfills all design rules, is the most challenging point for common equivalent plate theories (see Section 1). In case of DD, a simple post-processing procedure can be applied. Therefore, the panel thickness t_{lam} has only to be rounded onto the next whole multiple $\lceil r \rceil$ of the determined BB with a predefined ply thickness (Fig. 2).

$$\lceil r \rceil = \frac{t_{lam}}{4 \cdot t_{ply}} \tag{16}$$

Ensuring that homogeneity is satisfied for the stacking with the number of BB repeats, the condition of Eq. (5) is proven for each panel. If the stated condition is not full-filled, r is increased iteratively. In fact, this violation should occur very seldom for common aerospace structures, because homogeneity is usually already achieved with 3–4 BBs (see Section 2.1), which corresponds to a very low thickness.

3.3. Design criteria

In order to evaluate the implemented DD parameter subject to critical loading, suitable design criteria have to be applied on the laminate level. For strength, this can be obtained by superimposing a ply-based failure criterion for all ply orientations to obtain a so-called omni-envelope for the entire laminate [25]. The principal is shown in Fig. 3 for the T300/N5208 composite material, that is chosen for the design study later on. Specifically, in the present work a first-ply-failure (FPF) criterion is implemented according to [26], where the Tsai–Wu failure surface is applied to materials in strain space to determine the worst case for all possible ply angles. The envelope can be divided in two cases. For each case an elliptical form given in Eq. (17) has to be solved. The particular coefficients are given in Appendix A.

$$C_{ij}\varepsilon_i\varepsilon_j + RC_i + R^2C_0 = 0, \qquad i,j = I,II \tag{17}$$

R in Eq. (17) represents the strain exposure, where $R \leq 1$ means that the current strains are lower than the critical ones and no failure appear.

$$R = \frac{\varepsilon_{applied}}{\varepsilon_{crit}} \tag{18}$$

The highest root R from Eq. (17) gives the constraint value for optimization.

In addition to laminate strength, buckling stability is evaluated analytically within the applied optimization process, since it is a typical failure mode in composite shell structures. [28] gives for a simply-supported plate of length a and width b, under axial compression, the following expression for critical longitudinal stress resultant.

$$n_{x,crit} = k_x \cdot \frac{\pi^2}{b^2}\sqrt{D_{11}D_{22}} \tag{19}$$

$n_{x,crit}$ is the critical axial compression stress resultant. k_x is the buckling factor, which depends on stiffness and geometry related coefficients, which are given in Appendix B.

For the critical shear stress resultant $n_{s,crit}$, no exact closed form solution exists. Some approximations exist for infinitesimal long plates. The Aeronautical Engineering Handbook [29] provides a method to determine the buckling factor for a shear loaded rectangular plate to determine k_s. The relevant coefficients are provided in Appendix B.

$$n_{s,crit} = k_s \cdot \left(\frac{\pi}{b}\right)^2 \sqrt[4]{D_{11}D_{22}^3} \tag{20}$$

If axial and shear loads exist, [28] provides an interaction formula for coupled loads.

$$R_x + R_s^2 \leq 1 \tag{21}$$

where R represents the ratio of applied and the critical load of the corresponding load type. The aforementioned methods provide a reliable design of composite structures considering the most relevant design criteria.

4. Least weight design studies

4.1. Wing box use case

The proposed DD formulation is implemented to a gradient-based optimization process and applied to a simplified wing box model. This benchmark model is first suggested by [30] and used for various composite optimization studies, as summarized in [10]. There, a simple rectangular wing box represents the structural model (Fig. 4). The upper and lower shell is divided into nine design regions each and 18 in total (Fig. 5). These regions are defined by four equally distributed spars and ribs, that are fixed to a shear layup of $[(\pm 45°)_{22}]$. The wing

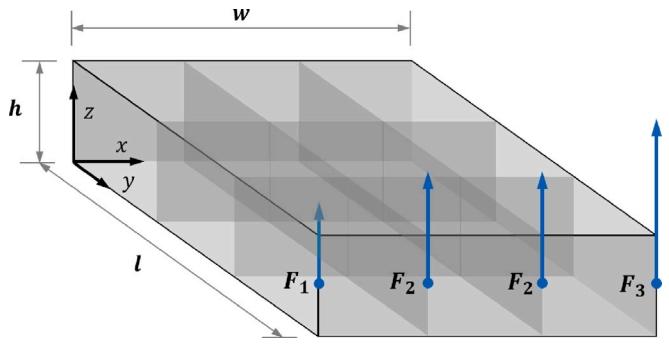

Fig. 4. Wing box topological layout, with: l = 3543 mm; w = 2240 mm; h = 381 mm; F_1 = 90 009.77 N; F_2 = 187 888.44 N; F_3 = 380 176.16 N.

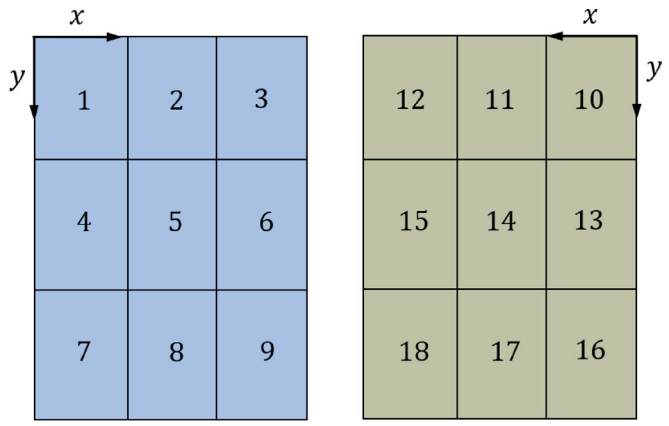

Fig. 5. Panels resp. design regions on upper shell (left) and lower shell (right).

box is clamped at the root section and loaded on the wing tip. The objective is to minimize the total mass of the upper and lower shell.

The constants of the used graphite–epoxy composite material are listed in Table 1. Most of the aforementioned studies use maximum strain allowables for the failure evaluation, which appear unusually high, especially for transverse failure strain with 0.029 and without distinction between tension and compression. Thus, the present work applies the constants as used in [8] and in accordance with [27].

For the suggested optimization strategy, a CPACS model [31] is used as input, containing the parameterized wing box. The CPACS file is available from an open repository [32]. Based on this data, a finite-element model is generated for the internal analysis. More detailed information about the used mesh and boundary conditions can be found in [10]. With this model, optimizations of the total mass are carried out as described hereafter.

4.2. Problem formulation and optimization strategy

On the basis of the continuous DD formulation an optimization strategy is presented, using the lightworks framework, as introduced in [10].

The objective to be minimized is the structural mass collected from an assembly of simply supported panel units for each rib bay of the wing box use case (Fig. 5). These panels represent a design region to be adjusted with the help of the design variables, subject to critical strength and buckling load, as well as feasibility-related criteria and upper and lower bounds. An overview of the optimization problems solved are given in Table 2.

A panel is characterized through its dimensions and constitutive properties according to the CLT. The ABD-stiffness is composed by the continuous DD formulation. Hence, for the DD specific optimization

Table 1
Composite material properties used for rectangular wing box use case according to literature.

Constants	Unit	T300/N5208
E_1	(GPa)	181
E_2	(GPa)	10.3
ν_{12}	(−)	0.27
G_{12}	(GPa)	7.17
ρ	(kg m^{-3})	1760
$X_t = X_c$	(MPa)	1500
Y_t	(MPa)	40
Y_c	(MPa)	246
S	(MPa)	68

problem, the design variable vector denotes: $\{x\}_{DD} := \{\Phi_m, \Psi_m, t_{lam}{}_n \mid m = 1,2;\ n = 1,\dots,18\}$. whereas the DD angles Φ and Ψ are optimized for each assembly structure m, which is the upper and lower shell, the thickness t_{lam} is adjusted for each panel n. In sum, the wing box problem results into 22 variables.

Furthermore, the DD design is compared to a conventional Quad laminate design. Therefore, LP are used as continuous design variables (Eq. (10)), as it is implemented in lightworks. Assuming symmetric and balanced Quad laminates (0°, 90° and ±45°-plies), the total number of 12 LP can be reduced to 5 for the complete design space. Hence, together with the thickness, the design variable vector is given with: $\{x\}_{Quad} := \{V_1^A{}_n, V_2^A{}_n, V_1^D{}_n, V_2^D{}_n, V_3^D{}_n, t_{lam}{}_n \mid n = 1,\dots,18\}$. Collecting 6 variables for each panel denotes 108 in total for the wing box use case.

The load state of a panel is provided by an external solver. Therefore, the panels ABD-stiffnesses are mapped on an analysis model. In this study, the b2000++ finite element solver is used. With this, the displacement field is solved and external loads are transformed into internal loads $\{N\}$, $\{M\}$. Then, the obtained internal loads are transformed on the panels in order to evaluate the design criteria, as outlined in Section 3.3. In addition, the LP require a feasible domain to consider respective laminate design rules, as already visualized section-wise in Fig. 1. The implemented approach to create the 5-dimensional design space for Quad laminates as a convex hull on the basis of hyperplanes is given in [12].

The optimization of both equivalent plate formulations is done on the basis of numerical sensitivities $\frac{\partial f}{\partial x_j}$ and $\frac{\partial g_i}{\partial x_j}$. For the calculation the complex step method is used, which is based on a truncated Taylor series expansion, assuming an imaginary step of a parameter. This allows a numerical exact gradient determination [33]. The gradient processing is the most expensive process step within the computation and therefore distributed to available parallel cores. For the numerical optimization, the SNOPT optimizer [34] with the open pyOptSparse package is used. All calculations are performed on an Intel(R) Xeon(R) CPU E5-2690 v3 @ 2.60 GHz with 12 physical cores. All 12 cores are used in parallel to evaluate the gradients.

4.3. Optimization results

4.3.1. DD design sensitivity analysis

The result of the proposed optimization approach is analyzed and verified within a sensitivity study. Basically, the wing box upper shell is driven through buckling stability due to the combined bending and torsional loading. This leads generally to a shear dominant BB with $[\pm 48, \pm 48]$ for the DD upper shell. On the lower shell, strength is critical at the wing root (panels 10–14), caused by the upward bending moment. At the wing tip shear buckling is critical again such that the found angles of $[0, \pm 46]$ are a compromise, that balances both constraints.

The found optimal BB's for the upper and lower shell are supported by contour plots of the respective design space in Figs. 6 and 7. The plots are obtained using only the panel thicknesses for optimization. Thereby, the objective function is analyzed generating a minimum mass

Table 2
Optimization problem descriptions.

	Constraint/Variable	Description	Quantity		Bounds
			DD	LP	
Minimize	m	Mass of upper and lower covers	1	1	
With respect to	t	Thickness of each panel	18	18	$(0, inf)$
	Ψ	First double double angle	2	–	$[0, 90]$
	Φ	Second double double angle	2	–	$[0, 90]$
	V_l^m	Lamination parameters	–	90	$[-1, 1]$
Total parameters			**22**	**108**	
Subject to	$g_{stability}$	Panel buckling	18	18	<0
	$g_{strength}$	Strength Omni-FPF	270	270	<0
	g_{lp}	LP design space	–	882	<0
Total constraints			**288**	**1170**	

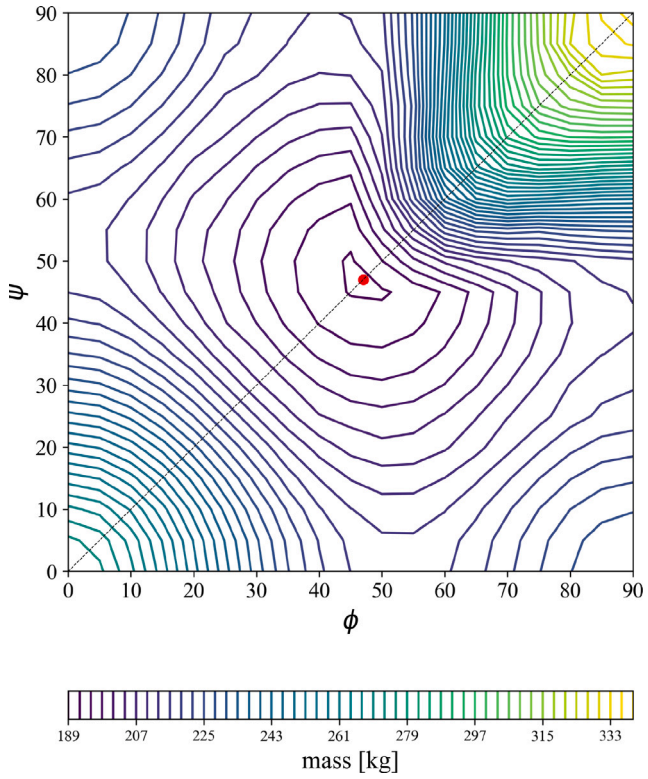

Fig. 6. Upper shell mass subject to the BB, derived from thickness optimizations with optimal BB for lower shell $[0, \pm 46]$.

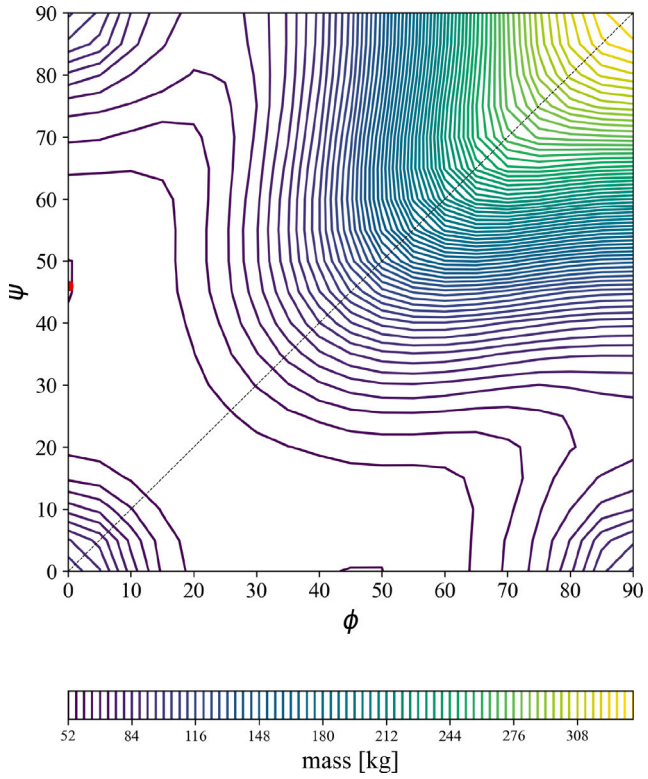

Fig. 7. Lower shell mass subject to the BB, derived from thickness optimizations with optimal BB for upper shell $[\pm 48, \pm 48]$.

result within 5° increments for Φ and Ψ, where the BB of the respective other shell is fixed to its optimum. The mass contours over Φ and Ψ in the range of 0°–90° show a continuous design space, that provides a global optimum, which is required for gradient-based algorithms. It can be seen, that the region of optimality of the lower shell is quite flat (Fig. 7). In this range, different DD angle combinations lead to only small mass deviations, which opens possibilities for multi-objective optimization.

A second requirement which allows for the usage of gradients is the robustness against varying initialization and perturbations. This is analyzed starting optimizations from different DD angle combinations within 5° increments. Thereby, the mass optimum is reliably achieved for 92% of all starting values, with a deviation of the optimal mass of $\Delta f \leq \pm 2$ kg and the highest constraint value being in the range of $c < 0.01$. A poorer convergence reveals at the outer boundaries of the DD angle space, where some starting values needs more iterations or even do not converge (Fig. 8). However, a robust optimization process is verified for the suggested parameterization. It has to be noted that this response is analyzed specifically for one use case, representing a typical wing design problem, using a specific optimization algorithm and gradient determination procedure (see Section 4.1).

4.3.2. Comparison of quad and DD parameterized wing box optimization

In order to compare the DD design to a conventional Quad design, an optimization was carried out, using the LP parameterization as outlined in Section 4.3. The optimized laminate properties of both designs are visualized with the polar distribution of the A_{11} in-plane stiffness (Fig. 9). For DD the BBs are the same for upper shell and lower shell, such that the polar properties are constant for all panels. For the LP model the stacking is allowed to be adjusted individually for each panel which leads to a more specific stiffness subject to its panel load state.

On Fig. 10 the thickness distribution of the LP and the DD approach is plotted. Here, it can be seen that the panel DD stiffness is a compromise for the total structure. The thicknesses of the LP variant exhausts its design freedom with higher thickness amplitudes locally, whereas the DD thickness is smoother distributed. An overview of both results is given in Table 3

Table 3
Results of DD and Quad laminate wing box optimization, with c being the maximum constraint value, either buckling stability, or laminate strength or ply strength respectively.

Panel	DD laminate					Quad laminate						
	$[\Phi,\Psi]$	Continuous		Discrete		V_1^A	V_2^A	V_1^D	V_2^D	V_3^D	t_{lam}	c
		t_{lam}	c	$\lceil t_{lam} \rceil$	c							
1		16.7	1e−10	17.0	−6e−2	0.16	−0.43	−0.01	−0.95	0.00	13.1	−5e−13
2		17.5	1e−10	18.0	−7e−2	0.50	−0.68	−0.01	−1.00	0.00	16.7	−2e−13
3		17.1	2e−10	17,5	−8e−3	−0.17	−0.68	−0.01	−1.00	0.00	20.4	−4e−14
4		14.0	2e−10	14.0	−2e−2	0.16	−0.43	−0.01	−0.95	0.00	11.1	7e−14
5	48, 48	14.7	1e−10	15.0	−5e−2	0.05	−0.68	−0.01	−1.00	0.00	14.1	−4e−14
6		14.0	2e−10	14.5	−9e−2	−0.17	−0.68	−0.01	−1.00	0.00	17.1	2e−14
7		9.9	3e−10	10.0	−6e−2	−0.06	−0.43	−0.01	−0.95	0.00	8.4	−5e−13
8		9.6	3e−10	10.0	−1e−1	−0.17	−0.68	−0.01	−1.00	0.00	9.0	−4e−13
9		10.0	2e−10	10.0	−3e−2	−0.28	−0.45	−0.03	−0.95	0.00	11.9	−3e−13
10		4.6	−2e−11	5.0	−1e−1	0.58	0.22	0.36	−0.05	−0.44	2.2	−1e−16
11		4.2	−1e−2	4.5	−1e−1	0.70	0.43	0.30	−0.22	0.13	1.0	5e−17
12		4.3	−1e−11	4.5	−5e−2	0.84	0.62	0.66	0.28	0.17	7.6	5e−17
13		3.5	−1e−10	3.5	−9e−2	0.39	0.16	−0.15	−0.25	0.18	1.9	−1e−16
14	0, 46	3.0	1e−11	3.0	−8e−2	0.50	0.40	−0.06	−0.03	0.12	1.0	−9e−13
15		3.1	−3e−11	3.5	−3e−2	0.72	0.40	0.51	−0.03	0.28	5.1	−5e−13
16		4.1	−4e−12	4.5	−3e−1	0.20	0.23	−0.46	0.16	0.13	2.4	−9e−13
17		4.7	−4e−11	5.0	−2e−1	0.34	0.26	−0.27	0.00	0.13	4.0	−4e−13
18		4.7	−5e−11	5.0	−2e−1	0.54	0.31	0.05	−0.25	0.17	4.0	2e−14

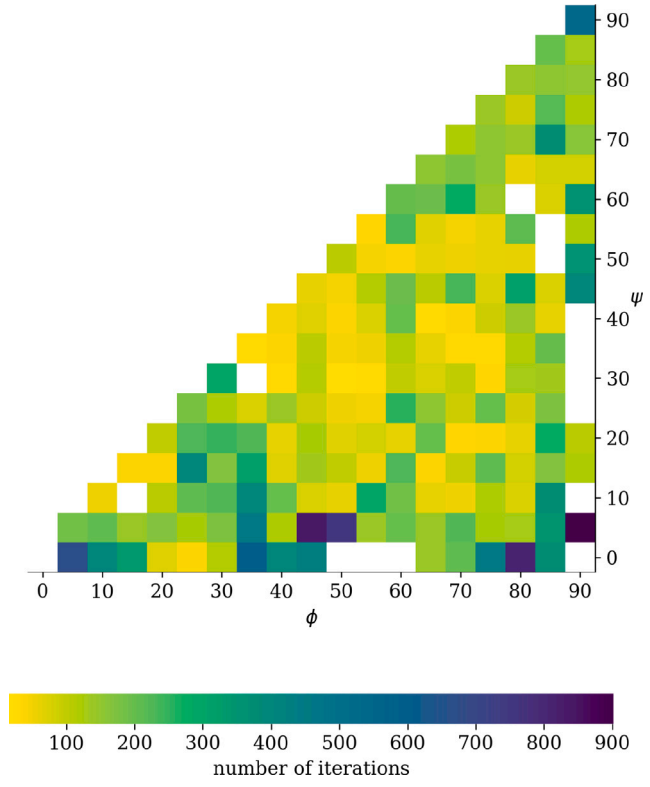

Fig. 8. Iterations needed to convergence dependent on varying starting angle combinations (blank points are not converged).

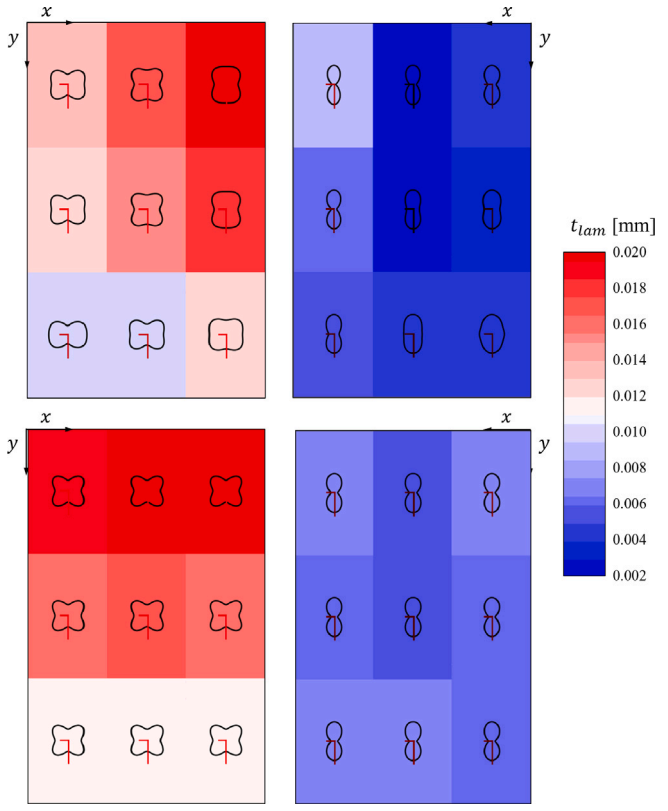

Fig. 9. Optimized thicknesses and polar distribution of A_{11} of LP (top) and DD (bottom) on upper shell (left) and lower shell (right).

The lower design freedom of the DD parameterization w.r.t the total structure leads to a wing box mass of 247.7 kg, which is 6.5% higher compared to the Quad laminate design with 232.5 kg.

For the subsequent step of rounding the thickness to whole multiples of BBs a common ply thickness of 0.125 mm is chosen. In order to verify intact plies after this transformation, one constraint analysis is run subsequently with a new structural model of these discrete stackings. There, instead of the laminate strength envelope, the Tsai–Wu criterion is evaluated on the ply level. It can be shown that all constraints have a higher reserve after transformation into a discrete stacking, due to the rounded thickness $\lceil t_{lam} \rceil$ (Table 3). The BB rounding adds 3% more mass to the continuous DD result. In case of LP stiffness the stacking sequence retrieval is much more complex, as already discussed in Section 1. Especially, the consideration of discrete blending between adjacent panels induces deviations of the continuously formulated Quad stackings, which is given for the DD approach. In [14] the retrieved layup including blending leads to 5.5% additional mass compared to an optimally designed continuous laminate on the example of the so-called "horse shoe" problem. Assuming this mass

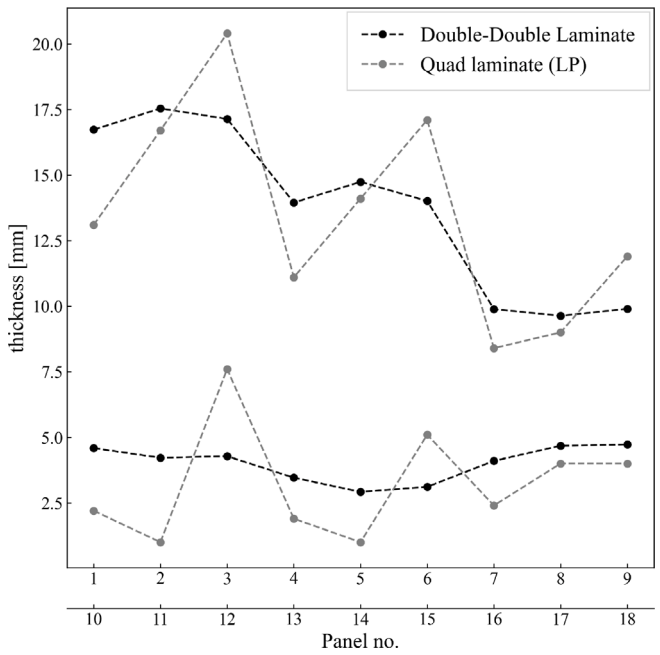

Fig. 10. Comparison of distributed thicknesses of Quad and DD design for upper shell (upper curves) and lower shell (lower curves).

increase, the difference between DD and Quad yields 4.5% higher mass for DD.

A comparison of the computational performance is done w.r.t. the different parameterization approaches. Where the Quad laminate needs 5 LP together with the thickness, the DD plate can be depicted by two angles and the thickness, as stated in Section 4.2. The lower amount of design variables also lowers the number of constraints and especially the number of gradients ($\frac{\partial f}{\partial x_j}$, $\frac{\partial g_i}{\partial x_j}$), which accounts for the most expensive step of the computation. In consequence, the DD structural design optimization is much more efficient. The mean time to calculate the DD gradients amounts to 10 s, whereas the LP problem takes 48 s.

5. Conclusion

In the present contribution, a continuous equivalent plate is suggested, which depicts the properties of a DD laminate. It is shown how this approach can be implemented and used for structural optimization of a composite wing box use case. A robust convergence against varying starting values to a global optimum is verified for the usage of gradients. It is recommended to start from a BB with some offset to the DD angle boundaries. In comparison with a common Quad laminate, the DD design reveals a higher weight. Whereas the DD design space is generally comparable to Quad laminates, the mass gains are caused by the blending approach that requires the same BB for an assembly of design regions, e.g. a wing shell. Hence, the Quad-based design is specific for each individual design region and therefore lighter. In the specific case of the academic wing box example, the higher mass is the price to pay for a much simplified design. Opposed to other continuous composite models, the derived DD structure is discrete and feasible by definition, which provides increased maturity in early design phases. Additionally, the reduction of design variables, that is enabled by the DD plate formulation, provides large computational savings. This effect grows with the amount of design regions of a real wing design problem, which makes it even more advantageous, especially in expensive MDO workflows. Additional benefits through the induced simplicity of DD reveal in detailed aircraft wing design including cut-outs, connection points and interface regions, e.g. when local support patches can be added without unbalancing the laminate mechanics. On the other hand further mass gains could occur for DD in more complex load scenarios, where a more specific tailoring of the composite is advantageous. However, in sum, the DD design strategy combines the lightweight benefits of composites, providing a tailored stiffness, with the simplicity of isotropic materials and can be represented with continuous design variables.

CRediT authorship contribution statement

David Zerbst: Writing – original draft, Software, Methodology, Formal analysis, Conceptualization. **Lennart Tönjes:** Writing – review & editing, Software, Methodology, Formal analysis. **Sascha Dähne:** Writing – review & editing, Writing – original draft, Methodology, Conceptualization. **Edgar Werthen:** Writing – review & editing, Writing – original draft, Methodology, Conceptualization. **Erik Kappel:** Writing – original draft, Conceptualization. **Christian Hühne:** Writing – review & editing, Funding acquisition.

Declaration of competing interest

The authors declare that they have no known competing financial interests or personal relationships that could have appeared to influence the work reported in this paper.

Acknowledgments

The author acknowledges funding from the German Federal Ministry of Economic Affairs and Climate Action (BMWK) under project number 20W1910D (Composite Tragflügel Neuer Technologie). Coauthor Edgar Werthen acknowledges funding from the German Research Foundation (DFG) under Germany's Collaborative Research Center – CRC 1463, project number 434502799 (Integrated design and operation methodology for offshore megastructures). Coauthor Erik Kappel acknowledges funding from the German Federal Ministry for Economic Affairs and Climate Action (BMWK) under project number 20A2201E (AirTiMe-DLR).

Appendix A. Strength coefficients

The coefficients of Tsai–Wu failure criterion:

$$u_1 = G_{22} - \frac{G_{22}}{2};\ u_2 = \frac{G_{66}}{2};\ u_3 = 2G_{12} - 2(G_{22} - \frac{G_{66}}{2})$$
$$u_4 = G_{11} - 2G_{12} + G_{22} - G_{66};\ u5 = G_2;\ u_6 = G_1 - G_2,$$

where G_i and $G_{ij}(i, j = 1, 2, \dots, 6)$ are the coefficients of Tsai–Wu failure criterion in terms of principal strains:

$$G_{11} - Q_{11}^2 F_{11} + Q_{12}^2 F_{22} + 2F_{12}Q_{11}Q_{12}$$
$$G_{22} = Q_{12}^2 F_{11} + Q_{22}^2 F_{22} + 2F_{12}Q_{12}Q_{22}$$
$$G_1 = Q_{11}F_1 + Q_{12}F_2; \quad G_2 = Q_{12}F_1 + Q_{22}F_2$$
$$G_{12} = Q_{11}Q_{12}F_{11} + Q_{12}Q_{22}F_{22} + F_{12}Q_{12}^2 + F_{12}Q_{11}Q_{22}$$
$$G_{66} = 4Q_{66}^2 F_{66}$$

The coefficients of Tsai–Wu expressed as an ellipse equation in terms of principal strains (Eq. (17)) for the materials with a critical second order envelope are:

$$C_0 = -\frac{(1/4)u_6^2}{u4} - 1;\ C_I = -\frac{(1/2)u_3 u_6}{u_4} + u_5;\ C_{II} = C_I;$$
$$C_{I\,I} = -\frac{(1/4)u_3^2}{u_4} + u_2 + u_1;\ C_{I\,II} = u_1 - \frac{(1/4)u_3^2}{u_4};$$
$$C_{II\,II} = -\frac{(1/4)u_3^2}{u_4} + u_2 + u_1$$

For the fourth order envelope as the critical envelope, these coefficients for each of the two branches of the envelope are used:

$$C_0(1) = C_0(2) = -1;\ C_I(1) = C_{II}(2) = u_5$$
$$C_{II}(1) = C_I(2) = u_6 + u_5;\ C_{I\,I}(1) = C_{II\,II}(2) = u_2 + u_1$$
$$C_{I\,II}(1) = C_{I\,II}(2) = (1/2)u_3 + u_1$$
$$C_{II\,II}(1) = C_{II}(2) = u_2 + u_1 + u_3 + u_4.$$

Appendix B. Buckling coefficients

Coefficients for compression buckling.

$$n_{x,cr} = k_x \cdot \frac{\pi^2}{b^2}\sqrt{D_{11}D_{22}}$$
$$k_x = \frac{m^2}{\bar{\alpha}^2} + \frac{\bar{\alpha}^2}{m^2} + 2\beta$$
$$\bar{\alpha} = \frac{a}{b} \cdot \sqrt[4]{\frac{D_{22}}{D_{11}}}$$
$$\beta = \frac{D_{12}+2D_{33}}{\sqrt{D_{11}D_{22}}}$$

An interpolation of the curves from the Aeronautical Engineering Handbook was done by the author based on polynomial functions.

$$k_s = a_2 \cdot \bar{\alpha}^{-2} + a_1 \cdot \bar{\alpha}^{-1} + a_0$$
$$a_2 = 2,7 \cdot \beta + 0,94\,,$$
$$a_1 = 0,34$$
$$a_0 = -0,15\beta^2 + 2,15 \cdot \beta + 3.34$$

Data availability

The raw data required to reproduce these findings are available to download from https://doi.org/10.5281/zenodo.10302734.

References

[1] Gray JS, Hwang JT, Martins JRRA, Moore KT, Naylor BA. OpenMDAO: An open-source framework for multidisciplinary design, analysis, and optimization. Struct Multidiscip Optim 2019;59(4):1075–104. http://dx.doi.org/10.1007/s00158-019-02211-z, URL: http://link.springer.com/10.1007/s00158-019-02211-z.

[2] Ilic C, Merle A, Ronzheimer A, Abu-Zurayk M, Jepsen J, Leitner M, Schulze M, Schuster A, Petsch M, Gottfried S. Cybermatrix a novel approach to computationally and collaboration intensive multidisciplinary optimization for transport aircraft design. In: Dillmann A, Heller G, Krämer E, Wagner C, Tropea C, Jakirlic S, editors. New results in numerical and experimental fluid mechanics XII. Notes on numerical fluid mechanics and multidisciplinary design, vol. 142, Cham: Springer; 2020, p. 37–47. http://dx.doi.org/10.1007/978-3-030-25253-3_4.

[3] Martins JRRA, Kennedy GJ. Enabling large-scale multidisciplinary design optimization through adjoint sensitivity analysis. Struct Multidiscip Optim 2021. http://dx.doi.org/10.1007/s00158-021-03067-y.

[4] Abu-Zurayk M, Merle A, Ilic C, Keye S, Goertz S, Schulze M, Klimmek T, Kaiser C, Quero D, Häßy J, Becker R, Fröhler B, Hartmann J. Sensitivity-based multifidelity multidisciplinary optimization of a powered aircraft subject to a comprehensive set of loads. In: AIAA AVIATION 2020 FORUM. AIAA AVIATION forum, American Institute of Aeronautics and Astronautics; 2020, http://dx.doi.org/10.2514/6.2020-3168, URL: https://arc.aiaa.org/doi/10.2514/6.2020-3168.

[5] Nikbakt S, Kamarian S, Shakeri M. A review on optimization of composite structures part I: Laminated composites. Compos Struct 2018;195:158–85.

[6] Ghadge R, Ghorpade R, Joshi S. Multi-disciplinary design optimization of composite structures: A review. Compos Struct 2022;280:114875. http://dx.doi.org/10.1016/j.compstruct.2021.114875.

[7] Wunderlich T, Dähne S. Aeroelastic tailoring of an NLF forward swept wing. CEAS Aeronaut J 2017;8(3):461–79. http://dx.doi.org/10.1007/s13272-017-0251-6.

[8] Scardaoni MP, Montemurro M. A general global-local modelling framework for the deterministic optimisation of composite structures. Struct Multidiscip Optim 2020;62(4):1927–49. http://dx.doi.org/10.1007/s00158-020-02586-4.

[9] Albazzan MA, Harik R, Tatting BF, Gürdal Z. Efficient design optimization of non-conventional laminated composites using lamination parameters: A state of the art. Compos Struct 2019;209:362–74. http://dx.doi.org/10.1016/j.compstruct.2018.10.095.

[10] Dähne S, Werthen E, Zerbst D, Tönjes L, Traub H, Hühne C. Lightworks, a scientific research framework for the design of stiffened composite-panel structures using gradient-based optimization. Struct Multidiscip Optim 2024;67(5):70. http://dx.doi.org/10.1007/s00158-024-03783-1.

[11] Diaconu C, Sato M, Sekine H. Layup optimization of symmetrically laminated thick plates for fundamental frequencies using lamination parameters. Struct Multidiscip Optim 2002;24(4):302–11. http://dx.doi.org/10.1007/s00158-002-0241-z.

[12] Werthen E, Dähne S. Design- and manufacturing constraints witin the gradient based optimization of a composite aircraft wingbox. In: 6th airframe structural design conference. 2018.

[13] Macquart T, Maes V, Bordogna MT, Pirrera A, Weaver PM. Optimisation of composite structures – enforcing the feasibility of lamination parameter constraints with computationally-efficient maps. Compos Struct 2018;192:605–15. http://dx.doi.org/10.1016/j.compstruct.2018.03.049.

[14] Scardaoni MP, Montemurro M, Panettieri E, Catapano A. New blending constraints and a stack-recovery strategy for the multi-scale design of composite laminates. Struct Multidiscip Optim 2021;63(2):741–66. http://dx.doi.org/10.1007/s00158-020-02725-x.

[15] Viquerat AD. A continuation-based method for finding laminated composite stacking sequences. Compos Struct 2020;238:111872. http://dx.doi.org/10.1016/j.compstruct.2020.111872.

[16] Sprengholz M, Traub H, Sinapius M, Dähne S, Hühne C. Rapid transformation of lamination parameters into stacking sequences. Compos Struct 2021;276:114514. http://dx.doi.org/10.1016/j.compstruct.2021.114514.

[17] Fedon N, Weaver PM, Pirrera A, Macquart T. A method using beam search to design the lay-ups of composite laminates with many plies. Composites C 2021;4:100072. http://dx.doi.org/10.1016/j.jcomc.2020.100072, URL: https://www.sciencedirect.com/science/article/pii/S2666682020300724.

[18] Tsai SW. Double–double: New family of composite laminates. AIAA J 2021;59(11):4293–305. http://dx.doi.org/10.2514/1.J060659, arXiv:https://doi.org/10.2514/1.J060659.

[19] Tsai SW, Falzon BG, Aravand A, editors. DOUBLE–DOUBLE simplifying the design and manufacture of composite laminates. 2nd ed.. Stanford, CA: by Composites Design Group, Department of Aeronautics and Astronautics, Stanford University; 2023, 94305-4035.

[20] Nettles A. Basic mechanics of laminated composite plates—NASA reference publication 1351. Technical report, NASA; 1994.

[21] Tsai SW, Melo JDD. Composite materials design and testing—Unlocking mystery with invariants. Stanford University; 2015.

[22] Tsai SW, Pagano NJ. Invariant properties of composite materials. 1968.

[23] Zhao K, Kennedy D, Miravete A, Tsai SW, Featherston CA, Liu X. Defining the design space for double–double laminates by considering homogenization criterion. AIAA J 2023;61(7):3190–203. http://dx.doi.org/10.2514/1.J062639, arXiv:https://doi.org/10.2514/1.J062639.

[24] Bailie JA, Ley RP, Pasricha A. A summary and review of composite laminate design guidelines. Technical report, Northrop Grumman; 1997.

[25] Kappel E. Double–double laminates for aerospace applications—Finding best laminates for given load sets. Composites C 2022;8:100244.

[26] Khani A, Ijsselmuiden ST, Abdalla MM, Gürdal Z. Design of variable stiffness panels for maximum strength using lamination parameters. Composites B 2011;42(3):546–52. http://dx.doi.org/10.1016/j.compositesb.2010.11.005.

[27] Tsai S, Melo J. Composite materials design and testing: Unlocking mystery with invariants. Composites Design Group; 2015, URL: https://books.google.de/books?id=ykBrrgEACAAJ.

[28] Wiedemann J. Leichtbau elemente und konstruktion. zweite Auflage ed.. Springer-Verlag; 2007.

[29] Structural Analysis working group I. Luftfahrttechnisches Handbuch für strukturberechnung (HSB). IASB (Industrie Ausschuss Struktur Berechnungsunterlagen); 2009, Backup Publisher: DASA-Airbus, Bremen, Prof. L. Schwarmann, in German and English available at technical information library (TIB) at Hannover.

[30] Liu B, Haftka R, Akgün M. Two-level composite wing structural optimization using response surfaces. Struct Multidiscip Optim 2000;20(2):87–96. http://dx.doi.org/10.1007/s001580050140.

[31] Alder M, Moerland E, Jepsen J, Nagel B. Recent advances in establishing a common language for aircraft design with CPACS. Technical Report, DLR; 2020, doi:https://elib.dlr.de/134341/.

[32] Dähne S, Zerbst D. CPACS for rectangular box wing. 2023, http://dx.doi.org/10.5281/zenodo.10302734.

[33] Martins JRRA, Sturdza P, Alonso JJ. The complex-step derivative approximation. ACM Trans Math Software 2003;29(3):245–62. http://dx.doi.org/10.1145/838250.838251, URL: http://doi.acm.org/10.1145/838250.838251, place: New York, NY, USA Publisher: ACM.

[34] Gill PE, Murray W, Saunders MA. SNOPT: An SQP algorithm for large-scale constrained optimization. SIAM Rev 2005;47(1):99–131. http://dx.doi.org/10.1137/S0036144504446096.